2023 62nd IEEE Conference on Decision and Control (CDC)
December 13-15, 2023. Marina Bay Sands, Singapore

Near Collision and Controllability Analysis of Nonlinear Optimal Velocity Follow-the-Leader Dynamical Model In Traffic Flow

Hossein Nick Zinat Matin[1] and Maria Laura Delle Monache [1]

Abstract— **This paper examines the optimal velocity follow-the-leader dynamics, a microscopic traffic model, and explores different aspects of the dynamical model, with particular emphasis on collision analysis. More precisely, we present a rigorous boundary-layer analysis of the model which provides a careful understanding of the behavior of the dynamics in trade-off with the singularity of the model at collision.**

I. Introduction and Related Works

The emergence of autonomous driving technologies such as adaptive cruise control and self-driving systems has created different theoretical challenges in modeling and analysis of the governing dynamics of the traffic flow.

Traffic flow dynamics has been a widely studied research area for decades, with literature devoted to various models based on macroscopic, mesoscopic, and microscopic descriptions of traffic flow [1]. The microscopic class of dynamics considers individual vehicles and their interaction. The earliest car following models date back to the works of [2], [3], [4], [5]. Nonlinear follow-the-leader dynamics can be traced back to [6] and [7] among others. The celebrated Optimal Velocity (OV) dynamical model was introduced and analyzed in [8], [9], [10] and numerous following studies. In this paper, we consider the Optimal Velocity Follow-the-Leader (OVFL) dynamical model which is shown to possess favorable properties both from a practical and theoretical point of view [11], [12], [13], [14], [15], [16].

The optimal velocity part of the OVFL model with a positive coefficient defines a target velocity based on the distance between each vehicle and its preceding one. Comparing the target and the current velocities, the acceleration/deceleration will be encouraged by the OV model. The follow-the-leader term explains the force that tries to match the vehicle's velocity with the preceding one. As the instantaneous relaxation time (i.e. $(x_{n-1}-x_n)/\beta$ in (1)) decreases, a singularity occurs at collision. Understanding the interaction between such a singularity and the behavior of OVFL dynamics near collision is the main focus of this paper.

Stability analysis of platoon of vehicles following (1) has been studied from various points of view such as string stability, [5], [10], [17], [18], [19], [20], [21]. Analysis of collision has been addressed from different standing points in some prior works. In a simulation-based study, [22] investigates the likelihood of collision as a consequence of drivers' reaction time. A Lyapunov-based analysis in a neighborhood of the equilibrium point has been studied in [23], [11]. Nonlinear stability analysis and collision avoidance based on the safe distance is studied in [24] for the OV model.

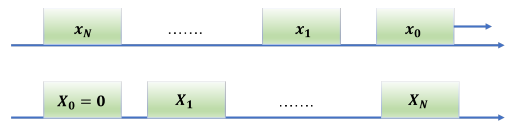

Fig. 1: The first illustration shows the position and direction of the vehicles. The second illustration depicts the relative position $X_n = x_0 - x_n$.

Focus and Contribution. In contrast to the stability-based analysis of OVFL dynamics, in this paper, we are interested in the analysis of collision (e.g. in a platoon of connected autonomous vehicles which are governed by such a dynamical model). In other words, our main focus is on understanding the interplay between the behavior of the OVFL dynamics and the singularity introduced in (1) at collision, through a careful and mathematically rigorous investigation.

Our boundary-layer analysis results are strongly dependent on the initial values which allow us to study the effect of singularity when the vehicles are in a near-collision region. Such analytical understanding is crucial in analyzing the behavior of the system in real-world conditions such as in the presence of noise and perturbation. In such conditions, sooner or later any physical system will be pushed into various states. Therefore it is necessary and insightful to understand the deterministic behavior of the system in the proximity of critical states.

As a consequence of our analysis, we show that the collision in the system does not happen and hence the system is well-posed. In addition, our analysis applies to multiple-vehicle which extends the results of [13].

The organization of this paper is as follows. We start by introducing the dynamical model. Then, we prove some essential properties of the dynamics between the first two vehicles which will be used in the analysis of the other following vehicles. Then, we study the behavior of the trajectory of other vehicles with respect to that of the first two and we show the main result of the paper.

II. Mathematical Model

We consider $N+1$ number of vehicles and each vehicle $n = 0, 1, \cdots, N$ has position x_n and velocity $y_n = \dot{x}_n$ such that $x_N < x_{N-1} < \cdots < x_0$ (see Figure 1). We assume that the first vehicle is moving with a constant velocity $\bar{v}$; i.e.

[1] Hossein Nick Zinat Matin and Maria Laura Delle Monache are with the Department of Civil and Environmental Engineering, University of California, Berkeley, h-matin@berkeley.edu, mldellemonache@berkeley.edu

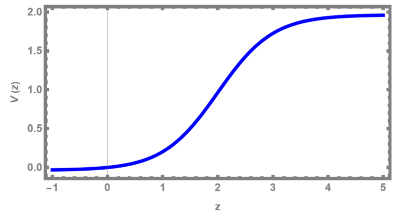

Fig. 2: Function V in (2).

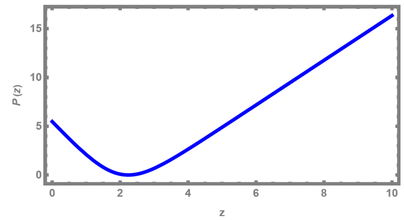

Fig. 3: Potential P (7) and Hamiltonian H (6) along the trajectory $(X_1(t), Y_1(t))$.

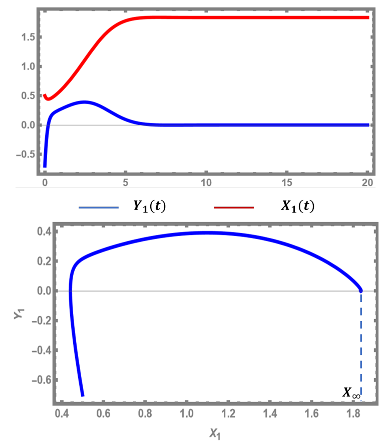

Fig. 4: Trajectory of the first two vehicles. The top plot shows the trajectory of $t \mapsto X_1(t)$ and $t \mapsto Y_1(t))$ separately. The bottom plot show the orbit of this dynamic for $\alpha = 2$, $\beta = 1$, $\bar{v} = 0.8$, $(X_{1,\circ}, Y_{1,\circ}) = (0.5, -0.7)$.

$\dot{x}_0(t) = y_0(t) = \bar{v}$ with the initial value $(x_\circ, y_\circ)$. For $n \geq 1$

$$(\text{OVFL}) \begin{cases} \dot{x}_n(t) = y_n(t) \\ \dot{y}_n(t) = \alpha \{V(x_{n-1} - x_n) + y_n(t))\} + \beta \frac{y_{n-1} - y_n}{(x_{n-1} - x_n)^2} \\ (x_n(0), y_n(0)) = (x_{n,\circ}, y_{n,\circ}) \end{cases} \quad (1)$$

where function V is monotonically increasing, bounded, and Lipschitz continuous function. In this paper, we consider

$$V(x) \overset{\text{def}}{=} \tanh(x-2) - \tanh(-2); \quad (2)$$

see Figure 2. We define $V(\infty) = 1.96$ as the scaled maximum possible speed and we ignore the length of vehicles as it doesn't affect the analysis. Therefore,

$$y_n(t) \in [0, V(\infty)), \quad n \in \{0, \cdots, N\}, \quad t \geq 0. \quad (3)$$

For simplicity of the analysis, we define the change of variable in (1)

$$X_n(t) \overset{\text{def}}{=} x_0(t) - x_n(t), \quad n = 1, \cdots, N$$
$$Y_n(t) \overset{\text{def}}{=} y_0(t) - y_n(t) = \bar{v} - y_n(t), \quad n = 1, \cdots, N$$

Consequently, the dynamics of (1) can be rewritten as

$$\begin{cases} \dot{X}_n(t) = Y_n(t) \\ \dot{Y}_n(t) = -\alpha \{V(X_n - X_{n-1}) + Y_n(t) - \bar{v}\} - \beta \frac{Y_n - Y_{n-1}}{(X_n - X_{n-1})^2} \\ (X_n(0), Y_n(0)) = (X_{n,\circ}, Y_{n,\circ}) \end{cases} \quad (4)$$

for $n \in \{1, \cdots, N\}$ with the convention that $X_0 = Y_0 = 0$. It should be noted that in (4) we have that $X_N > \cdots > X_1 > X_0 = 0$; see Figure 1. In addition, following (3), we have that

$$Y_n(t) \in (\bar{v} - V(\infty), \bar{v}], \quad t \geq 0. \quad (5)$$

This is in particular important in choosing the initial values of the dynamics. The dynamical system (4) has a unique equilibrium solution when all the vehicles are equidistantly located and moving with the same velocity [10], [21]. Mathematically, for each $n \in \{1, \cdots, N\}$

$$(X_n^\infty, Y_n^\infty) = (nV^{-1}(\bar{v}), 0) = (nX_\infty, 0)$$
$$X_\infty = V^{-1}(\bar{v}) = 2 + \tanh^{-1}(v_\circ + \tanh(-2)),$$

III. Dynamics of the First Two Vehicles

First, we need to understand the interaction between the first two vehicles carefully.

A. Hamiltonian and Boundedness of Solution

In this section, we consider $N = 1$ in (4), the dynamics between the first two vehicles. Following [13], first we recall few properties of the dynamics of $(X_1(t), Y_1(t))$. The main properties of the dynamics of $(X_1(t), Y_1(t))$ can be obtained by defining the Hamiltonian function

$$H(x, y) \overset{\text{def}}{=} \frac{1}{2} y^2 + P(x) \qquad (x, y) \in \mathbb{R}^2 \quad (6)$$

with the potential function

$$P(x) \overset{\text{def}}{=} \alpha \int_{x' = X_\infty}^{x} \{V(x') - \bar{v}\} \, dx'; \qquad x \in \mathbb{R}. \quad (7)$$

Using (6), we can show that the solution (X_1, Y_1) is bounded. In particular, it is straightforward to see

$$\dot{H}(X_1(t), Y_1(t)) = -\left\{\alpha + \frac{\beta}{X_1(t)^2}\right\} Y_1(t)^2 \leq 0 \quad (8)$$

By the definition of H, we have that

$$\begin{aligned} &\tfrac{1}{2} Y_1^2(t) \leq H(X_1(t), Y_1(t)) \leq h_\circ \\ &h_\circ \overset{\text{def}}{=} H(X_{1,\circ}, Y_{1,\circ}) \end{aligned} \quad (9)$$

Therefore,

$$|Y_1(t)| \leq \bar{y} \overset{\text{def}}{=} \sqrt{2h_\circ}, \quad X_1(t) \leq \bar{x} \overset{\text{def}}{=} h_\circ, \quad t \geq 0. \quad (10)$$

Finally, it is shown that the solution $X_1(t)$ never hit zero which can be interpreted as no collision between the first two vehicles. In particular,

$$X_1(t) \geq \delta_1, \quad t \geq 0 \quad (11)$$

where, the lowerbound $\delta_1 = \delta_1(X_{1,\circ}, Y_{1,\circ})$ depends on the initial values of the system. Figure 4 shows the trajectory of the dynamical model for the first two vehicles. Now, we need to develop some more properties of the trajectory of flow $(X_1(t), Y_1(t))$.

Remark 3.1: Using (10) and (11), set $(0,\bar{x}] \times [-\bar{y}, \bar{y}]$ is positively invariant with respect to the flow $(X_1(t), Y_1(t))$ and has a compact closure. Furthermore, (8) precludes a periodic orbit. Therefore, an application of the Poincaré-Bendixon theorem, suggests that the equilibrium solution $(X_\infty, 0)$ is globally asymptotically stable.

In this paper, we are mainly concerned with the boundary-layer analysis of the system near collision (the situation that can happen, for instance, as a result of instantaneous perturbation in the system; like sudden braking of the leading vehicles which propagates). In other words, we are interested in the case that the distance between the corresponding consecutive vehicles becomes relatively small. In particular, we consider the initial values $\Delta X_{n,\circ} < X_\infty$, for the respective $n \in \{1, \cdots, N\}$.

In addition, suppose that $Y_{1,\circ} < 0$. Fix a time $T > 0$. Since $X_{1,\circ} < X_\infty$, the dynamics of (4) for $N = 1$ suggest that $\dot{Y}_1(t) > 0$ for $t \in (0, \varepsilon_\circ)$; some neighborhood of time zero. On the other hand, since the $X_{1,\circ}$ is relatively small, the dominant term in the dynamics of $\dot{Y}_1$ in (4) is $-\beta Y_1(t)/(X_1(t))^2$ for $t \in (0, \varepsilon_\circ)$. Hence, for sufficiently large β, $Y_1(\bar{t}) > 0$ for some $\bar{t} < T$ (see Figure 4). Therefore, in this paper, we consider the case of $Y_{1,\circ} > 0$; otherwise, the same analysis follows after shifting the initial time to $\bar{t}$.

Moreover, the interaction between two consecutive vehicles depends on their relative speed, i.e. $Y_2 - Y_1$ (rather than merely the relative velocity Y_1 of the leading vehicle) which will be analyzed in its full generality. In particular, the most interesting case for the purpose of our boundary layer analysis will be $Y_n - Y_{n-1} < 0$, $n \geq 2$, which implies that the following vehicle is moving faster than the leading one. This can potentially result in a collision. We will discuss this case in detail in the next section.

B. Controlling the Behavior of the Dynamics by Controlling the Parameters

In this section, we study the behavior of the trajectory of $t \mapsto Y_1(t)$ for $(X_{1,\circ}, Y_{1,\circ}) \in (0, X_\infty] \times \mathbb{R}_+$. We define

$$\mathscr{T}_\infty \stackrel{\text{def}}{=} \inf\{t \geq 0 : X_1(t) = X_\infty\} \tag{12}$$

as the first time for which the trajectory $t \mapsto X_1(t)$, starting from the initial data $(X_{1,\circ}, Y_{1,\circ})$, approaches X_∞. The change of variables $u \stackrel{\text{def}}{=} x - X_\infty$ and $v \stackrel{\text{def}}{=} y$ help us standardize the stability analysis by translating the equilibrium point to the origin. The Hamiltonian can be rewritten as

$$\begin{aligned} H(u,v) &= \tfrac{1}{2}v^2 + \tilde{P}(u) \stackrel{\text{def}}{=} \tfrac{1}{2}v^2 + \alpha \int_0^u \{V(u' + X_\infty) - \bar{v}\}\, du' \\ \frac{dH}{dt}(u(t), v(t)) &= -\left(\alpha + \frac{\beta}{(u(t) + X_\infty)^2}\right) v^2(t). \end{aligned} \tag{13}$$

The main result of this section expresses that by controlling the parameters α and β we can control the behavior of the trajectory $t \mapsto Y_1(t)$. In particular,

Theorem 3.2: Starting from $(X_{1,\circ}, Y_{1,\circ}) \in (0, X_\infty] \times \mathbb{R}_+$, for sufficiently large values of α and β, we have that

$$\limsup_{t \nearrow \mathscr{T}_\infty} v(t) = 0.$$

This implies that by controlling α and β, the flow $Y_1(t)$ will be absorbed to the equilibrium point as $t \nearrow \mathscr{T}_\infty$. We postpone the proof of this theorem until some preliminary results are established. The following lemmas explain the behavior of the trajectory $t \mapsto Y_1(t)$ around the equilibrium point. Figure 5 is provided as a graphical aide to the proofs.

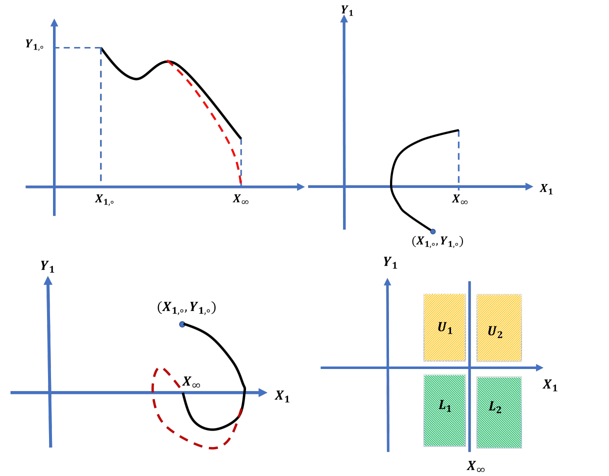

Fig. 5: The behavior of the trajectory for the different cases of initial values $(X_{1,\circ}, Y_{1,\circ})$.

Lemma 3.3: The set $U_1 \stackrel{\text{def}}{=} \{(x,y) : x < X_\infty, y \in \mathbb{R}_+\}$ is invariant with respect to the trajectory $[0, \mathscr{T}_\infty) \ni t \mapsto (X_1(t), Y_1(t))$. In other words, if $(X_{1,\circ}, Y_{1,\circ}) \in U_1$, then $Y_1(t) > 0$ for $t \in [0, \mathscr{T}_\infty)$.

Proof: We use the proof by contradiction to show the result. Suppose that there exists a time $t_\circ < \mathscr{T}_\infty$ such that $Y_1(t_\circ) = 0$. By the continuity of the solution, we have that $\dot{Y}_1(t_\circ) < 0$. On the other hand,

$$\begin{aligned} \dot{Y}_1(t_\circ) &= -\alpha\{V(X_1(t_\circ)) - \bar{v} + Y_1(t_\circ)\} - \beta \frac{Y_1(t_\circ)}{(X_1(t_\circ))^2} \\ &= -\alpha\{V(X_1(t_\circ)) - \bar{v}\} > 0 \end{aligned}$$

where the last inequality holds since $X_1(t_\circ) < X_\infty$. But this is a contradiction and hence the result follows (see Figure 5). ■

In a similar manner, one can discuss the behavior of the integral curve around the equilibrium point.

We like to show that the rate of convergence of the trajectory $(X_1(t), Y_1(t))$ to the equilibrium point can be controlled by controlling the parameters α and β.

Lemma 3.4: Let's define the domain $\mathscr{C} \stackrel{\text{def}}{=} (\delta_1 - X_\infty, \bar{x} - X_\infty) \times \mathbb{R}$ (see (10) and (11) and the definition of u, v before (13)) which contains the equilibrium point. There exists constants $\underline{k}$ and $\bar{k}$ such that

$$\underline{k}\|U\|^2 \leq H(u,v) \leq \bar{k}\|U\|^2, \quad U = (u,v)^\top \in \mathscr{C}$$

Proof: The right-hand side inequality is by Lipschitz continuity of function V and the fact that $\bar{v} = V(X_\infty)$ and for $\bar{k} \stackrel{\text{def}}{=} \max\left\{\frac{1}{2}, \alpha\right\}$. To see the left-hand side of the inequality, we note that function $\tilde{P}$ (as in (13)) is a convex function (see the illustration P of Figure 3 and consider that the equilibrium point is shifted to the origin) and in addition, over the domain $\bar{\mathscr{C}}$, the closure, we have

$$\tilde{P}''(u) = \alpha V'(u + X_\infty) \geq \alpha k_{(14)} > 0 \tag{14}$$

for some constant $k_{(14)} > 0$. Therefore, $\tilde{P}$ is strongly convex on $\mathscr{C}$ which implies that

$$\tilde{P}(u) \geq \tilde{P}(0) + \tilde{P}'(0)u + \frac{\alpha k_{(14)}}{2} u^2$$

Since $\tilde{P}(0) = \tilde{P}'(0) = 0$, we have that

$$H(u,v) = \tfrac{1}{2}v^2 + \tilde{P}(u) \geq \tfrac{1}{2}v^2 + \frac{\alpha k_{(14)}}{2}u^2 \geq \underline{k}\|U\|^2 \tag{15}$$

for $\underline{k} \stackrel{\text{def}}{=} \min\left\{\frac{1}{2}, \frac{\alpha k_{(14)}}{2}\right\}$. This completes the proof. ■

For the proof of Theorem 3.2, with a slight abuse of notation, we consider $\mathscr{T}_\infty$ as in (12) to denote the time that trajectory $t \mapsto u(t)$ approaches the origin (which is the equilibrium point here). *Proof:* [of Theorem 3.2] Let us fix $\varepsilon > 0$ such that $\text{Ball}((0,0)^\top, \varepsilon)$ be the region of attraction (for exponential stability) of the origin in the linearized model; see Remark 3.1. We recall Lemma 3.3 and we define

$$\mathscr{T}_\infty^\varepsilon \stackrel{\text{def}}{=} \inf\{t < \mathscr{T}_\infty : u(t) < \varepsilon/3\}, \tag{16}$$

If for some values of α and β

$$v(t) < \varepsilon, \quad t \in [\mathscr{T}_\infty^\varepsilon, \mathscr{T}_\infty),$$

i.e. is already in the domain of attraction, then the claim follows by exponential convergence of the linearized problem. Suppose on the contrary that for all values of α and β, $v(t) \geq \varepsilon$ on $[\mathscr{T}_\infty^\varepsilon, \mathscr{T}_\infty)$. Then over the domain $\mathscr{C}$

$$\left(\alpha + \frac{\beta}{(u(t)+X_\infty)^2}\right)v^2(t) \geq \tfrac{1}{2}\left(\alpha + \frac{\beta}{\bar{x}^2}\right)v^2(t) + \tfrac{1}{2}\left(\alpha + \frac{\beta}{\bar{x}^2}\right)\varepsilon^2$$
$$\geq \tfrac{1}{2}\left(\alpha + \frac{\beta}{\bar{x}^2}\right)\left\|(u(t),v(t))^\top\right\|^2$$

for $t \in [\mathscr{T}_\infty^\varepsilon, \mathscr{T}_\infty)$, and where the last inequality is by (16). Using (13), we have that over $t \in [\mathscr{T}_\infty^\varepsilon, \mathscr{T}_\infty)$

$$\dot{H}(u(t),v(t)) \leq -K_{(17)}\left\|(u(t),v(t))^\top\right\|^2, \tag{17}$$

where, $K_{(17)} \stackrel{\text{def}}{=} \frac{1}{2}\left(\alpha + \frac{\beta}{\bar{x}^2}\right)$.

Using Lemma 3.4 and (17), we can write

$$\dot{H}(u(t),v(t)) \leq -\frac{K_{(17)}}{\bar{k}}H(u(t),v(t)), \quad t \in [\mathscr{T}_\infty^\varepsilon, \mathscr{T}_\infty).$$

Using Gronwall's inequality, we get

$$H(u(t),v(t)) \leq H(u(\mathscr{T}_\infty^\varepsilon), v(\mathscr{T}_\infty^\varepsilon))\exp\left\{-\frac{K_{(17)}}{\bar{k}}t\right\},$$

for $t \in [\mathscr{T}_\infty^\varepsilon, \mathscr{T}_\infty)$. Once more, using Lemma 3.4, we will have

$$\begin{aligned}\left\|(u(t),v(t))^\top\right\|^2 &\leq \frac{1}{\underline{k}}H(u(t),v(t)) \\ &\leq \frac{1}{\underline{k}}H(u(\mathscr{T}_\infty^\varepsilon), v(\mathscr{T}_\infty^\varepsilon))\exp\left\{-\frac{K_{(17)}}{\bar{k}}t\right\} \\ &\leq \frac{h_\circ}{\underline{k}}\exp\left\{-\frac{K_{(17)}}{\bar{k}}t\right\}, \quad t \in [\mathscr{T}_\infty^\varepsilon, \mathscr{T}_\infty),\end{aligned}$$

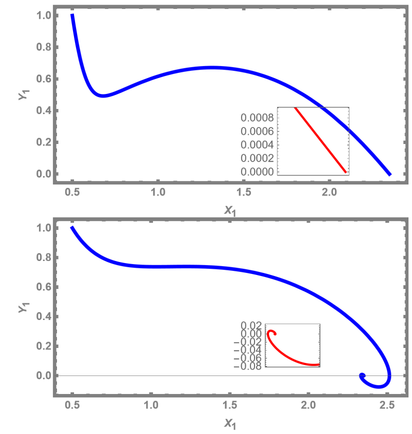

Fig. 6: The first figure is for $\alpha = 3$, $\beta = 2$ and it converges to the rest point. The second figure is with respect to $\alpha = \beta = 1$. Hence for relatively small α and β, the integral curve will spin around the equilibrium point before it is absorbed. The red curves zoom into the behavior of the trajectories near the equilibrium point. Other parameters are $\bar{v} = 1.3$, $(X_{1,\circ}, Y_{1,\circ}) = (0.5, 1)$.

where the last inequality is from (8). But comparing $K_{(17)}$ and $\bar{k}$ shows that for sufficiently large values of α and β, $\left\|(u(t),v(t))^\top\right\| < \varepsilon$ for some $t \in (\mathscr{T}_\infty^\varepsilon, \mathscr{T}_\infty)$ which contradicts our initial assumption. Therefore, the statement of the theorem follows (see Figure 6). ■

IV. Dynamics of Other Vehicles

The analysis of the properties of the dynamics of interaction between vehicle n and $n-1$ for $n \geq 2$ requires an in-depth understanding of the interaction between vehicles $n-1$ and $n-2$ (the leading vehicles). In this section, using the results of section III, we will consider the interaction between vehicles n and $n-1$ for $n = 2$ (the interaction between vehicles two and three).

For the purpose of our analysis (in particular collision analysis), we need to work with the *difference* flow $(X_2 - X_1, Y_2 - Y_1)$ rather than the flow (X_2, Y_2). In particular, $X_2 - X_1 = 0$ means collision. Therefore, it would be reasonable to introduce the change of variables

$$\xi_1 \stackrel{\text{def}}{=} X_1, \quad \xi_2 \stackrel{\text{def}}{=} X_2 - X_1, \zeta_1 \stackrel{\text{def}}{=} Y_1 \quad \zeta_2 \stackrel{\text{def}}{=} Y_2 - Y_1,$$

and the difference dynamical model of (4) then reads

$$\begin{cases}\dot{\xi}_1 = \zeta_1 \\ \dot{\zeta}_1 = -\alpha\{V(\xi_1) - \bar{v}\} - \alpha\zeta_1 - \beta\frac{\zeta_1}{(\xi_1)^2} \\ \dot{\xi}_2 = \zeta_2 \\ \dot{\zeta}_2 = -\alpha\{V(\xi_2) - V(\xi_1)\} - \alpha\zeta_2 - \beta\left(\frac{\zeta_2}{(\xi_2)^2} - \frac{\zeta_1}{(\xi_1)^2}\right) \\ (\xi_1(0), \zeta_1(0)) = (\xi_{1,\circ}, \zeta_{1,\circ}) = (X_{1,\circ}, Y_{1,\circ}) \\ (\xi_2(0), \zeta_2(0)) = (\xi_{2,\circ}, \zeta_{2,\circ}) = (X_{2,\circ} - X_{1,\circ}, Y_{2,\circ} - Y_{1,\circ}).\end{cases} \tag{18}$$

First, we look at the existence of the solution of the dynamics of (18). We define the state space

$$\mathscr{D} \stackrel{\text{def}}{=} ((0,\infty) \times \mathbb{R})^2 \ni (\xi_{1,0}, \zeta_{1,0}, \xi_{2,0}, \zeta_{2,0}) \tag{19}$$

and the flow $\Xi \stackrel{\text{def}}{=} (\xi_1, \zeta_1, \xi_2, \zeta_2)$. From the abstract theory of dynamical systems, the solution of (18) exists on a maximal interval $[0, \mathscr{T}^c)$, for some $\mathscr{T}^c > 0$.

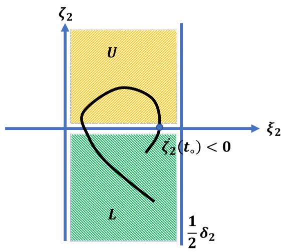

Fig. 7: Illustration of the proof discussions.

Assumption. We suppose that

$$\mathscr{T}^c < \infty. \tag{20}$$

We start with the implications of (20). As $t \nearrow \mathscr{T}^c$, the flow Ξ, either grows unbounded, or $\Xi \in \partial\mathscr{D}$. We recall that under the conditions of Theorem 3.2, ζ_1 vanishes at $\mathscr{T}_\infty$. Therefore, if $\mathscr{T}^c \geq \mathscr{T}_\infty$ then for $t \in [\mathscr{T}_\infty, \mathscr{T}^c)$ the dynamics $\dot{\zeta}_2$ in (18) will be the same as dynamics of $\dot{\zeta}_1$ and so the solution exists for all $t \geq \mathscr{T}_\infty$; i.e. $\mathscr{T}^c = \infty$. On the other hand, $\zeta_2 \to \pm\infty$ is prohibited by the properties of the dynamics and since $\xi_1(t) \notin \{0\}$, we must have

$$\lim_{t \nearrow \mathscr{T}^c} \xi_2(t) = 0, \tag{21}$$

i.e. $\mathscr{T}^c$ is the collision time.
Under such an assumption, there exists a time

$$\check{t} \overset{\textbf{def}}{=} \sup\left\{t < \mathscr{T}^c : \xi_2 > \tfrac{1}{2}\delta_2\right\}, \quad \delta_2 \overset{\textbf{def}}{=} \min\{\xi_{2,\circ}, \delta_1\} \tag{22}$$

where $\delta_1 < X_\infty$ is defined in (11). In other words, if the collision time is finite, then there should be a time $\check{t}$ after which the trajectory $\xi_2(t) \leq \frac{1}{2}\delta_2$, for $t \in [\check{t}, \mathscr{T}^c)$. We study the behavior of the $\dot{\zeta}_2$ in this region. The next result shows that in this region, $\zeta_2(t) < 0$; i.e. the follower vehicle is moving faster than the leading one.

Lemma 4.1: The Set $\mathscr{U} \overset{\textbf{def}}{=} \left\{(x,y) : x \in (0, \frac{1}{2}\delta_2), y \in \mathbb{R}_+\right\}$ is invariant with respect to the trajectory $t \in [\check{t}, \mathscr{T}^c) \mapsto (\xi_2(t), \zeta_2(t))$. In other words, if $\zeta_2(t) > 0$ for some $t \in [\check{t}, \mathscr{T}^c)$, then it must remain positive.

Proof: Figure 7 illustrates the proof argument. Suppose on the contrary that $\zeta_2(t) < 0$ for some $t \in [\check{t}, \mathscr{T}^c)$. This implies, by definition of $\check{t}$, there exists a time $t_\circ$ such that $\zeta_2(t_\circ) = 0$ and $\dot{\zeta}_2(t_\circ) < 0$. But using the dynamics of ζ_2 in (18) as well as (22), must have that

$$\dot{\zeta}_2(t_\circ) = -\alpha\left\{V(\xi_2(t_\circ)) - V(\xi_1(t_\circ)\right\} + \beta\frac{\zeta_1}{(\xi_1)^2} > 0,$$

which is a contradiction. ∎

Remark 4.2: Lemma 4.1 along with the assumption (20) shows in particular that $\zeta_2(t) < 0$ for $t \in [\check{t}, \mathscr{T}^c)$.

Lemma 4.3: For $t \in [\check{t}, \mathscr{T}^c)$, we have that

$$\dot{\zeta}_2(t) > 0.$$

Proof: Let's consider the dynamics of $\dot{\zeta}_2$ in (18). Then, (22) implies that $-\alpha\left\{V(\xi_2) - V(\xi_1)\right\} > 0$. Remark 4.2 show that $-\alpha\zeta_2 > 0$. Finally $\zeta_1 > 0$ implies that the last term should also be positive and this completes the proof. ∎

Proposition 4.4: Under the conditions of Theorem 3.2, $\mathscr{T}^c = \infty$. In other words, collision does not happen in the dynamical model (18).

Proof: The result of Lemma 4.3 (monotonicity of $\zeta_2(t)$) suggests that, given the trajectory of $t \mapsto (\xi_1(t), \zeta_1(t))$, we should be able to locally write

$$\xi_2(t) = \psi(\zeta_2(t)), \quad \text{for } t \in [\check{t}, \mathscr{T}^c), \tag{23}$$

for some function ψ which will be constructed below. Employing (18), we have that

$$\zeta_2 = \dot{\xi}_2 = \psi'(\zeta_2)\dot{\zeta}_2 = \psi'(\zeta_2)\Bigg\{ -\alpha\left\{V(\psi(\zeta_2)) - V(\xi_1)\right\} - \alpha\zeta_2 \\ - \beta\left(\frac{\zeta_2}{(\psi(\zeta_2))^2} - \frac{\zeta_1}{(\xi_1)^2}\right)\Bigg\}. \tag{24}$$

Furthermore, thanks to strictly monotone behavior, the function $\zeta_2 : [\check{t}, \mathscr{T}^c) \to [\check{\zeta}, \hat{\zeta})$, where $\check{\zeta} \overset{\textbf{def}}{=} \zeta_2(\check{t})$ and $\hat{\zeta} \overset{\textbf{def}}{=} \zeta_2(\mathscr{T}^c)$, is a diffeomorphism. Let $\theta \overset{\textbf{def}}{=} \zeta_2^{-1}$, the inverse function of ζ_2. Then, function ζ_1 on $[\check{t}, \mathscr{T}^c)$ can be presented as the smooth function $\zeta_1 \circ \theta$ on $[\check{\zeta}, \hat{\zeta})$ if $\mathscr{T}^c < \mathscr{T}_\infty$ and zero otherwise. A similar argument holds true for $\xi_1 \circ \theta$.
Let us now formalize the construction of ψ by extending the function θ smoothly on the domain $(-\infty, 0)$ and defining a function

$$\mathbf{g}(\zeta,\psi) \overset{\textbf{def}}{=} \frac{-\zeta}{\alpha\left\{V(\psi) - V(\xi_1(\theta(\zeta)))\right\} + \alpha\zeta + \beta\left(\frac{\zeta}{\psi^2} - \frac{\zeta_1(\theta(\zeta))}{(\xi_1(\theta(\zeta)))^2}\right)}$$

for $(\zeta, \psi) \in (-\infty, 0) \times (0, \delta_2)$, and $(\zeta_1, \xi_1) \in (0, \bar{y}) \times (\delta_1, X_\infty)$. Therefore, using (24), the dynamical model can be presented by

$$\psi'(\zeta) = \mathbf{g}(\zeta, \psi(\zeta)), \quad \psi(\check{\zeta}) = \xi_2(\check{t}) \tag{25}$$

where $\check{\zeta} \overset{\textbf{def}}{=} \zeta_2(\check{t})$ and $\xi_2(\check{t}) = \frac{1}{2}\delta_2$. Through such construction, the dynamics of (25) is well-defined and has a maximal interval of existence $(\mu_-, \mu_+) \subset (-\infty, 0)$ and contains the initial value $\check{\zeta}$. The construction (25) creates a barrier dynamics through comparison with which we can show $\xi_2 > 0$ on $[\check{t}, \mathscr{T}^c)$ (see (23)).

Theorem 4.5: We have that

$$\inf_{\bar{\zeta} \in [\check{\zeta}, \mu_+)} \psi(\bar{\zeta}) > 0.$$

Proof: Let's consider the definition of $\psi'(\zeta)$ in (25). We recall that $\zeta_1 > 0$ for $t \in [\check{t}, \mathscr{T}^c)$, and by construction $\psi(\zeta) < \delta_2 \leq \delta_1 < \xi_1$. This implies that

$$\psi'(\zeta) < 0, \quad \zeta \in [\check{\zeta}, \mu_+).$$

Dividing both sides of (25) by $\psi^2(\zeta)$, it is straightforward to see that

$$\frac{\psi'(\zeta)}{\psi^2(\zeta)} > \frac{-\zeta}{\text{Negative Terms} + \beta\zeta} > \frac{-\zeta}{\beta\zeta} = -\frac{1}{\beta}$$

on $[\check{\zeta}, \mu_+)$. Then, one can show that (see [13])

$$\inf_{u \in [\check{\zeta}, \mu_+)} \psi(u) \geq \inf_{u \in [\check{\zeta}, \mu_+)} \mathscr{R}(u) \geq \left\{ (\tfrac{1}{2}\delta_2)^{-1} + \frac{\check{\zeta}}{\beta} \right\}^{-1}. \tag{26}$$

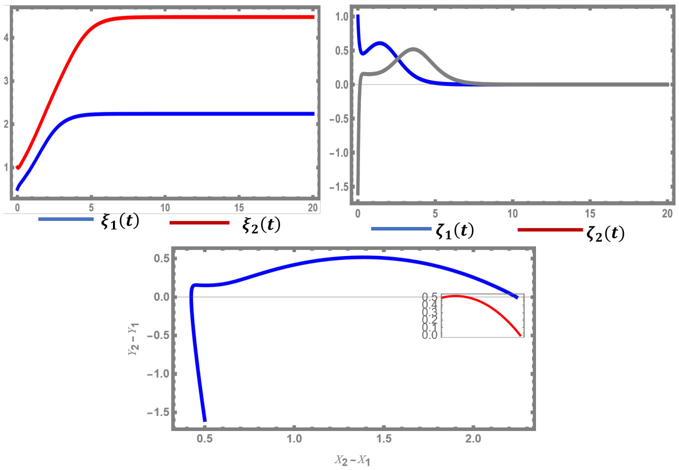

Fig. 8: Illustration of the trajectory of the dynamics between the first two and the second two vehicles.

This concludes the proof. ■

We conclude the proof of proposition 4.4, by showing that $\mu_+ = \hat{\zeta} = \zeta_2(\mathscr{T}^c)$. In other words, we show that the result of the Theorem 4.5 holds true for all $[\check{t}, \mathscr{T}^c)$ which in turn implies that $\mathscr{T}^c = \infty$. To do so, as mentioned before, $\zeta_2 : [\check{t}, \mathscr{T}^c) \to [\check{\zeta}, \hat{\zeta})$ is a homeomorphism. Therefore, we should have

$$\theta\big|_{[\check{t},\mathscr{T}^c)}\Big([\check{\zeta}, \mu_+) \cap [\check{\zeta}, \hat{\zeta})\Big) = [\check{t}, \mathscr{T}'),$$

for some $\mathscr{T}' \leq \mathscr{T}^c$ and we recall that $\theta = \zeta_2^{-1}$. From (25) $(\psi(\zeta), \zeta)$ solves the dynamics of (18) and hence must coincide with (ξ_2, ζ_2) on $[\check{t}, \mathscr{T}')$. The case of $\mathscr{T}' < \mathscr{T}^c$ is precluded by the behavior of the dynamics near the boundaries. For the case of, $\mathscr{T}' = \mathscr{T}^c$, $\lim_{t \nearrow \mathscr{T}^c} \psi(\zeta) = \lim_{t \nearrow \mathscr{T}^c} \xi_2 = 0$ which is prohibited by Theorem 4.5. This contradicts our main assumption (20). ■

V. Conclusions and Future Works

In this paper, we presented a rigorous boundary layer analysis of the OVFL dynamical model near collision. Such analysis provides an in-depth understanding of the behavior of the dynamics especially when the system is forced out of equilibrium. Understanding the interaction of the singularity and behavior of the dynamics near collision is fundamental both from a theoretical standpoint and in designing efficient systems, such as adaptive cruise controls.

This paper can be extended on several fronts. The theory can benefit from a broader definition of Hamiltonian which serves as a Lyapunov-type function to explain the boundedness and stability of the equilibrium solution. Utilizing this, further analysis is required to generalize the results in a rigorous way.

References

[1] M. Treiber and A. Kesting, "Traffic flow dynamics," *Traffic Flow Dynamics: Data, Models and Simulation, Springer-Verlag Berlin Heidelberg*, 2013.

[2] L. A. Pipes, "An operational analysis of traffic dynamics," *Journal of applied physics*, vol. 24, no. 3, pp. 274–281, 1953.

[3] G. F. Newell, "Nonlinear effects in the dynamics of car following," *Operations research*, vol. 9, no. 2, pp. 209–229, 1961.

[4] D. C. Gazis, R. Herman, and R. B. Potts, "Car-following theory of steady-state traffic flow," *Operations research*, vol. 7, no. 4, pp. 499–505, 1959.

[5] R. E. Chandler, R. Herman, and E. W. Montroll, "Traffic dynamics: studies in car following," *Operations research*, vol. 6, no. 2, pp. 165–184, 1958.

[6] R. Herman and R. B. Potts, "Single lane traffic theory and experiment," 1959.

[7] D. C. Gazis, R. Herman, and R. W. Rothery, "Nonlinear follow-the-leader models of traffic flow," *Operations research*, vol. 9, no. 4, pp. 545–567, 1961.

[8] M. Bando, K. Hasebe, A. Nakayama, A. Shibata, and Y. Sugiyama, "Dynamical model of traffic congestion and numerical simulation," *Physical review E*, vol. 51, no. 2, p. 1035, 1995.

[9] ——, "Structure stability of congestion in traffic dynamics," *Japan Journal of Industrial and Applied Mathematics*, vol. 11, no. 2, p. 203, 1994.

[10] M. Bando, K. Hasebe, K. Nakanishi, and A. Nakayama, "Analysis of optimal velocity model with explicit delay," *Physical Review E*, vol. 58, no. 5, p. 5429, 1998.

[11] A. Tordeux and A. Seyfried, "Collision-free nonuniform dynamics within continuous optimal velocity models," *Physical Review E*, vol. 90, no. 4, p. 042812, 2014.

[12] R. E. Stern, S. Cui, M. L. Delle Monache, R. Bhadani, M. Bunting, M. Churchill, N. Hamilton, R. Haulcy, H. Pohlmann, F. Wu, B. Piccoli, B. Siebold, J. Sprinkle, and D. B. Work, "Dissipation of stop-and-go waves via control of autonomous vehicles: Field experiments," *Transportation Research Part C: Emerging Technologies*, vol. 89, pp. 205–221, 2018.

[13] H. Nick Zinat Matin and R. B. Sowers, "Near-collision dynamics in a noisy car-following model," *SIAM Journal on Applied Mathematics*, vol. 82, no. 6, pp. 2080–2110, 2022.

[14] H. N. Z. Matin and R. B. Sowers, "Nonlinear optimal velocity car following dynamics (i): Approximation in presence of deterministic and stochastic perturbations," in *2020 American Control Conference (ACC)*. IEEE, 2020, pp. 410–415.

[15] H. Nick Zinat Matin and R. B. Sowers, "Nonlinear optimal velocity car following dynamics (ii): Rate of convergence in the presence of fast perturbation," in *American Control Conference*, 2020.

[16] M. L. Delle Monache, T. Liard, A. Rat, R. Stern, R. Badhani, B. Seibold, J. Sprinkle, D. B. Work, and B. Piccoli, "Feedback control algorithms for the dissipation of traffic waves with autonomous vehicles," in *Computational Intelligence and Optimization Methods for Control Engineering*. Springer, 2019, ch. 12, pp. 275–299. [Online]. Available: https://hal.inria.fr/hal-02335658

[17] E. Kometani and T. Sasaki, "On the stability of traffic flow (report-i)," *Journal of the Operations Research Society of Japan*, vol. 2, no. 1, pp. 11–26, 1958.

[18] R. E. Wilson and J. A. Ward, "Car-following models: fifty years of linear stability analysis–a mathematical perspective," *Transportation Planning and Technology*, vol. 34, no. 1, pp. 3–18, 2011.

[19] G. Gunter, D. Gloudemans, R. E. Stern, S. McQuade, R. Bhadani, M. Bunting, M. L. Delle Monache, R. Lysecky, B. Seibold, J. Sprinkle *et al.*, "Are commercially implemented adaptive cruise control systems string stable?" *IEEE Transactions on Intelligent Transportation Systems*, vol. 22, no. 11, pp. 6992–7003, 2020.

[20] V. Giammarino, S. Baldi, P. Frasca, and M. L. Delle Monache, "Traffic flow on a ring with a single autonomous vehicle: an interconnected stability perspective," *IEEE Transactions on Intelligent Transportation Systems*, vol. 22, no. 8, pp. 4998–5008, 4 2021. [Online]. Available: https://hal.inria.fr/hal-03011895/document

[21] M. Piu and G. Puppo, "Stability analysis of microscopic models for traffic flow with lane changing," *arXiv preprint arXiv:2203.00318*, 2022.

[22] L. Davis, "Modifications of the optimal velocity traffic model to include delay due to driver reaction time," *Physica A: Statistical Mechanics and its Applications*, vol. 319, pp. 557–567, 2003.

[23] ——, "Nonlinear dynamics of autonomous vehicles with limits on acceleration," *Physica A: Statistical Mechanics and its Applications*, vol. 405, pp. 128–139, 2014.

[24] C. Magnetti Gisolo, M. L. Delle Monache, F. Ferrante, and P. Frasca, "Nonlinear analysis of stability and safety of optimal velocity model vehicle groups on ring roads," *IEEE Transactions on Intelligent Transportation Systems*, vol. 23, no. 11, pp. 20 628–20 635, 11 2022.